

Intermittency and scaling property of band-pass-filtered signals in moderate-Reynolds-number turbulent flows

Tomoo Katsuyama, Yoshinori Horiuchi, and Ken-ichi Nagata

Department of Physics, Tokyo Metropolitan University, Minami-Ohsawa 1-1, Hachioji, Tokyo 192-03, Japan

(Received 9 September 1993)

The intermittency (multifractality) of turbulent velocity has been experimentally investigated through the frequency-band-pass-filtered velocity signals. In inertial range frequencies of the band-pass filter, the even number order moments of the signals show the scaling property on a nearly Gaussian distribution. The scaling exponents of the $2n$ th order moments are a nonlinear function of the order $2n$. The non-linearity means the frequency (scale) -dependent deviation of the statistics law of the signals are from Gaussian statistics. In dissipation range frequencies, the signals have no scaling property, and the deviation of the statistics law becomes much greater at higher frequencies. Such deviations of the statistics law are due to viscous effects, and reflect the breakdown of the self-similarity of turbulent velocity structure, that is to say its intermittent property.

PACS number(s): 47.27.-i, 02.50.-r, 03.40.Gc, 47.53.+n

I. INTRODUCTION

It is known that the “fine structure” of turbulent velocity fluctuations is spatially localized. The spottiness of the fine structure, first observed by Batchelor and Townsend [1], has been recognized to be the intermittent occurrence of high-frequency contribution in hot-wire anemometer output signals. They used a high-pass filter to extract a fine-scale signal from the anemometer output signal and defined the “flatness factor” of the high-pass-filtered signal as a quantitative measure of the intermittency.

The flatness factor of the first derivative of turbulent velocity has been measured by many workers [2–6]. The velocity derivative flatness factors were much larger than 3.0, and the amount by which it exceeds 3.0 is considered to be the degree of intermittency. By using a frequency-band-pass filter, Sandborn [7] found that the spottiness can be observed in the fine-scale components of turbulent velocity in the full turbulent part of a boundary layer.

Kennedy and Corrsin [8] experimentally showed that a high flatness factor does not necessarily imply intermittency. Kuo and Corrsin [9] proposed a direct measure of the intermittency. The direct measure is an intermittency factor defined as a fraction of time that a hot-wire probe “sees” a variable in a large amplitude state.

An important theory of intermediate and fine-structure turbulence was given by Kolmogorov’s (1941) local isotropy and similarity hypothesis [10]. Subsequently, Landau’s and Lifshitz’s comment [11] upon Kolmogorov’s 1941 theory attracted many investigators’ attention to the possible presence and importance of large fluctuations in the instantaneous energy dissipation rate ϵ . Thereafter, some attempts to include this fluctuation in theoretical analyses were performed by many workers [12–18].

In the modification of the Kolmogorov’s original similarity hypotheses, Oboukhov [12] and Kolmogorov [13] assumed that the logarithm of ϵ_r , the average energy dis-

sipation rate over a volume of linear dimension r , has a normal distribution function. They thereby arrived at a modified expression for the velocity structure function.

Anselmet *et al.* [19] measured the second- and higher-order moments of the structure function (velocity difference). Their experimental result supported neither the anticipated result from the log-normal model nor that from the β model (Frisch, Sulem, and Nelkin [18]).

Meaneveau and Sreenivasan [20] measured the r dependence of the q th-order moments of ϵ_r and obtained the generalized dimension D_q . They, as well as Anselmet *et al.*, determined experimentally that the simple (homogeneous) fractal models cannot explain the experimentally obtained q dependence of D_q . Hosokawa and Yamamoto [21] reached the same conclusion for isotropic turbulence by direct numerical simulations. To interpret those experimental results [19,20], several models based on multifractal notions were proposed by many workers [22–26].

She, Jackson, and Orszag [27] studied the statistics of velocity fluctuation in isotropic homogeneous turbulence decaying at moderately large Reynolds numbers, and they concluded that intermittency evaluated by the flatness factor is basically a dissipation range phenomenon. Their finding is that the high-amplitude events leading to the intermittency are embedded in a nearly Gaussian distribution, in contrast to the assumption of the simple phenomenological models.

Frequency-band-pass-filtered velocity signals directly reveal the intermittent phenomenon, which becomes more obvious at higher band-pass frequencies. So far, many workers have experimentally and theoretically researched the intermittency in various ways: through the band-pass (or high-pass) -filtered signals of turbulent velocity, the several-order moments of the velocity structure function, and the fluctuation of the local energy dissipation rate ϵ_r .

Using a multifractal approach, Benzi *et al.* [28] derived the probability distribution function (PDF) of the

velocity gradients in fully developed turbulence. They showed that the experimental data are in good agreement with the PDF predicted by the random β model [22]. Recently, another multifractal approach based on the so-called p model [20] was investigated by Kailasnath, Sreenivasan, and Stolovitzky [29]. They derived the PDF $p_{\Delta u}$ of velocity differences $\Delta u(r)$ between two spatial locations that are a distance r apart and experimentally showed that the tails of the PDF's are closely approximated by stretched exponential forms $p_{\Delta u} \propto \exp(-a|\Delta u|^m)$. Then, with decreasing r , the experimentally determined stretching exponent m decreased monotonically from 2 for the integral scale to 0.5 for the dissipation scale.

Discussions have been going on among many workers about the intermittency, and there is a common thread to the search. A common feature is the scale dependence of the statistics law in three-dimensional fully developed turbulence. All the discussions on the large flatness of the PDF, the fluctuations in the local energy dissipation rate, the scaling exponent of the structure function, and the stretched exponential form fitting to the tails of the PDF are related to the scale dependence of the statistics law. This suggests that the research into the multifractal nature through the statistics law is of greater importance.

In the present work, the scale dependence of the statistics law is experimentally investigated through the frequency-band-pass-filtered velocity signals in a wide frequency range from the inertial range to the dissipation range frequencies. Our experiment has an advantage in that the intermittent behavior of turbulent velocity can be investigated individually for the integral scale range, the inertial range, and the dissipation range.

II. EXPERIMENTAL CONDITIONS

Measurement was made for the following three turbulent air flows:

(1) Grid-generated turbulence. The open wind tunnel used has a test section 2 m long, 40×40 cm² in cross section. The grid was of a 1-cm-diam round rod, with mesh size $M = 4$ cm. Measurement was made at several distances from $10M$ to $30M$. The mean flow velocity U_0 was from 5 to 20 m/s at the measuring points.

(2) Turbulent jet flow from a square nozzle. Measurement was made for the two nozzles of cross sections 40×40 cm² and 10×10 cm², at distances above 15 times the length of the orifice side from the nozzles. The mean flow velocity was $U_0 = 3$ and 15 m/s at the measurement points on a jet axis.

(3) Turbulent wake behind a circular cylinder. The cylinders were of $D = 1, 3,$ and 5 cm in diameter and fixed in the orifice plane (40×40 cm² cross section). Measurement was made at distances from $40D$ to $200D$ on a center line of the wake. In the measurement points, the turbulence was in the initial period of its decay, and the measured energy-frequency spectra of turbulent velocity showed a universal form in their dissipation ranges.

Velocity measurement was made with a DANTEC 56C01 constant-temperature anemometer. A streamwise velocity component $u(t)$ was measured with an x-wire

probe ($5\text{-}\mu\text{m}$ -diam, 0.7-mm -long hot wires). The output signal of the anemometer was band-pass filtered. The band-pass filter was constructed by connecting a low-pass one and a high-pass one in a series, and their cutoff frequencies f_c were adjusted to the same value (see Fig. 1). This cutoff frequency f_c is a running midband frequency of the band-pass filter. The low- and high-pass filters were of an eight-pole Butterworth (maximum flat) characteristic, and had a rolloff rate of 48 dB/octave. The band-pass-filtered signal was digitized with 12-bit resolution at $10f_c$ sampling frequency.

The intermittency factors and PDF's of the band-pass-filtered signals were calculated from the records of data above 6×10^5 points. Indeed, to obtain an accurate form of the PDF's, we increased the number of points according to the degree of intermittency of the band-pass signals. The one-dimensional energy-frequency spectra of $u(t)$, $E_1(f)$ were obtained by performing the digital Fourier transform of its correlation functions measured with a digital autocorrelator, where f is a frequency.

The band-pass filters used had a 48 dB/octave rolloff rate (see Fig. 1). A frequency width of the band-pass filter, Δf , is required to be appropriately narrow, but the form of the response function of the filter by no means affects our conclusions which were obtained from the experimental results of the intermittency factor and the PDF. This was ascertained by the use of another band-pass filter with a faster rolloff rate of 135 dB/oct.

Since a frequency-band-pass filter works as an integral operator on its input signal, its output voltage at time t is determined based on its input signal history over a period from $t - \Delta t$ to t , Δt being roughly of the order of $1/\Delta f$. Incidentally, in the limit $\Delta f \rightarrow 0$, the output signal is determined on an infinitely long history; therefore, the output is technically indeterminable. From a mathematical viewpoint, the limit $\Delta f \rightarrow 0$ gives a Fourier component to be a constant amplitude sinusoidal wave. When Δf is too large, the output signal also has no intermittent aspect. The appearance of the intermittent facet requires that the band-pass filter should have an appropriately narrow finite bandwidth.

III. BAND-PASS FILTERED SIGNALS AND INTERMITTENCY FACTORS

Figure 2 shows the time records of band-pass-filtered-velocity signals $V(t; f_c)$ obtained in the jet flow of the

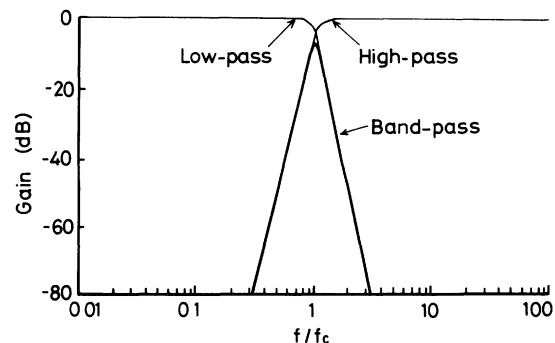


FIG. 1. Frequency response function of the band-pass filter.

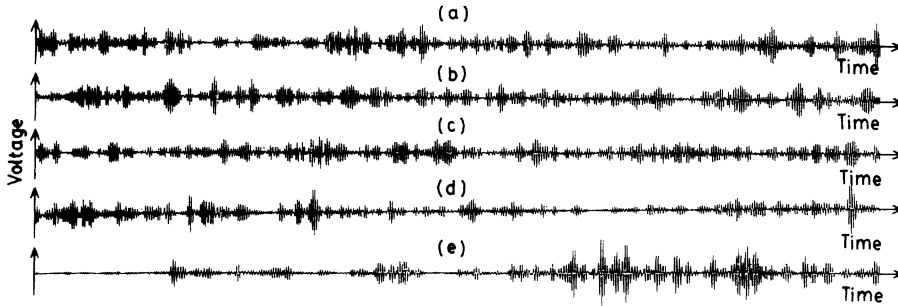


FIG. 2. Time records of band-pass-filtered velocity signals, (a) $f_c=0.07$ kHz, (b) 0.15 kHz, (c) 0.70 kHz, (d) 3.0 kHz, and (e) 10 kHz. The horizontal axes are a normalized time scale tf_c , and the vertical axes are an arbitrary scale.

turbulence Reynolds number $R_\lambda=270$, at the midband frequencies (a) $f_c=0.07$ kHz, (b) 0.15 kHz, (c) 0.70 kHz, (d) 3.0 kHz, and (e) 10 kHz. Here, the horizontal (time) and vertical (voltage) axes of each record have been scaled in the following way. The horizontal axes have been normalized by the periods $1/f_c$, so that the oscillations seen in each record have the same periods. The vertical axes have been scaled such that the maximum amplitudes of each record are roughly equal to each other.

Features seen in these records are categorized into the following two groups (see Fig. 2).

(A): In the low frequencies $f_c=0.07$, 0.15 and 0.70 kHz (a)–(c), which are located in the inertial range, these three records are similar to each other in the randomly amplitude-modulated sinusoidal oscillations. This means that turbulent velocity fluctuations can involve self-similar structures. There are almost no quiescent parts in oscillation.

(B): In the high frequencies $f_c=3.0$ and 10 kHz (d,e), which are located in the dissipation range, the oscillations have clearly quiescent parts, the growth of which is

recognized in the higher frequency. This feature is the spottiness in the fine structure of turbulent velocity.

The characteristics mentioned above are necessarily reflected in the PDF's of the band-pass signals. Figure 3 shows the PDF's $p(V)$ obtained from the band-pass signals $V(t;f_c)$ shown in Fig. 2, where the solid line curves represent Gaussian functions. At the lowest frequency (a), the PDF is almost Gaussian. The features of the PDF's are likewise classified into the above two categories: the PDF's in (a)–(c) are roughly Gaussian, but the ones in (d) and (e) are clearly non-Gaussian.

The PDF deviates from the Gaussian form with increasing f_c . The deviation from the Gaussian PDF arises in the large amplitudes of the oscillations and, with increasing f_c , extends to their smaller ones. Finally, as a consequence of the occurrence of the localized oscillations, the PDF becomes entirely non-Gaussian (Figs. 2 and 3).

According to Benzi *et al.* [28] and Kailasnath, Sreenivasan, and Stolovitzky [29], the PDF features can be expressed by the stretched exponential form $p(V) \propto \exp(-a|V|^m)$. Figure 4 shows a variation of the

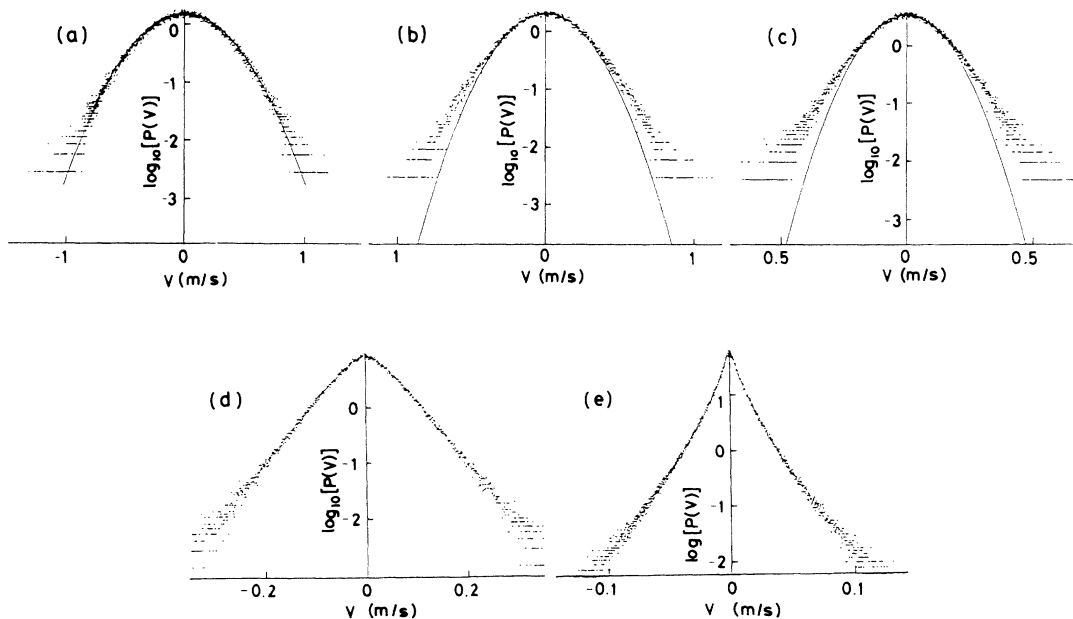


FIG. 3. PDF's of the band-pass signals shown in Fig. 2, (a) 0.07 kHz, (b) 0.15 kHz, (c) 0.70 kHz, (d) 3.0 kHz, and (e) 10 kHz, the solid line curves being Gaussian.

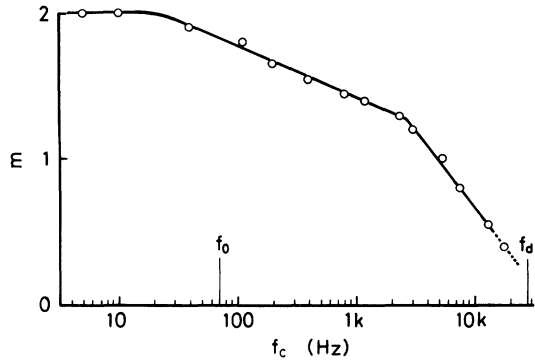


FIG. 4. Experimentally determined stretching exponent m in $p(V) \propto \exp(-a|V|^m)$, plotted as a function of f_c ; $R_\lambda = 270$ jet flow at $U_0 = 15$ m/s.

experimentally obtained stretching exponent m versus f_c . In the low frequencies ($f_c < 20$ Hz) in the integral scale range, the PDF's are almost Gaussian, and m is equal to 2. As f_c increases over 20 Hz, m decreases monotonically to 0.5. This decrease becomes more rapid in the dissipation range above 2 kHz. This behavior of m is different from that obtained by Kailasnath, Sreenivasan, and Stolovitzky for the velocity differences $\Delta u(r)$. In high frequencies over the frequency at which the smallest value 0.5 was obtained, $p(V)$ did not take the stretched exponential form expressed by a single exponent m . The behavior of m is discussed in detail in Sec. VI.

On the other hand, it is known that the deviation of the PDF from Gaussian statistics is quantitatively evaluated by the amount that the flatness exceeds 3.0. For the band-pass signals, the flatness factor F is given as

$$F = \frac{\langle [V(t; f_c)]^4 \rangle}{\langle [V(t; f_c)]^2 \rangle^2}, \quad (3.1)$$

where the symbol $\langle V^n \rangle$ stands for the time average of V^n : $\langle [V(t; f_c)]^n \rangle = (1/T) \int_0^T [V(t; f_c)]^n dt$, T being the whole length of the record of $V(t; f_c)$.

The signal $V(t; f_c)$ can be assumed to be an amplitude- and phase-modulated sinusoidal oscillation with a central frequency f_c (Fig. 2). If the amplitude and phase of the sinusoidal oscillation vary slowly in comparison with the period $1/f_c$, it is expressed as

$$V(t; f_c) = A(t) \sin[2\pi f_c t + \delta(t)]. \quad (3.2)$$

If $d\delta(t)/dt$ is very small in comparison with the angular frequency $2\pi f_c$, the substitution of Eq. (3.2) into Eq. (3.1) gives $F = (3/2) \langle A^4(t) \rangle / \langle A^2(t) \rangle^2$.

Next, let us suppose a perfectly amplitude-modulated binary signal, the amplitude of which takes a constant nonzero value in active parts and a zero value in residual inactive ones. Hereafter, we call such a binary signal an "on/off signal." If γ is a fraction of the "on" part with the constant amplitude oscillation, one obtains $F = 3/(2\gamma)$ for the on/off signal.

Here, suppose that a band-pass signal has been converted to an on/off signal according to the method of Kuo and Corrsin [9]. Then, γ is the "on" fraction. It is

possible to define γ with the flatness factor F of the original band-pass signal for a suitable setting of an on/off threshold level:

$$\gamma = \frac{3}{2} \frac{\langle [V(t; f_c)]^2 \rangle^2}{\langle [V(t; f_c)]^4 \rangle}. \quad (3.3)$$

Now, providing that $V(t; f_c)$ obeys the Gaussian statistics, we have $\gamma = 0.5$. However, even when $V(t; f_c)$ is non-Gaussian, there is a case where $\gamma = 0.5$. In other words, the on/off representation masks the statistics of $V(t; f_c)$. Hence, it is insufficient to define the degree of intermittency with the factor γ .

To supply this deficiency, it is necessary to take the higher-order moments of the PDF into account. We define the $2n$ th order moments of the band-pass signal, γ_{2n} ($n \geq 2$), which stand for the degree of intermittency:

$$\gamma_{2n} = \frac{(2n-1)!!}{2} \frac{\langle [V(t; f_c)]^{2n} \rangle}{\langle [V(t; f_c)]^2 \rangle^n} \quad \text{for } n = 2, 3, 4, \dots \quad (3.4)$$

where $(2n-1)!! = (2n-1)(2n-3) \dots 3 \cdot 1$. If $V(t; f_c)$ is a Gaussian variable, Eq. (3.4) has a constant value such that $\gamma_{2n} = 0.5$ for all $2n$.

IV. THE SCALING PROPERTY OF THE BAND-PASS SIGNAL

In extremely large Reynolds numbers, the Navier-Stokes equation for incompressible fluid is invariant under the scaling transformations

$$r \rightarrow \lambda r, \quad U \rightarrow \lambda^h U, \quad \text{and } t \rightarrow \lambda^{1-h} t, \quad (4.1)$$

where U is fluid velocity at a time space (t, r) , and λ is a positive real number. The scaling exponent h is an arbitrary real number. For fully developed turbulence, the scaling transformation invariance (4.1) is guaranteed in a statistical sense (Frisch [30]), and it is an attribute of the nonlinear dynamics of the Navier-Stokes equation in the limit of inviscosity.

Let $u(t)$ be the streamwise component of the turbulent velocity. Hereafter, the output voltage fluctuation of the anemometer to sense temporal variations of $u(t)$ is denoted in terms of the same notation $u(t)$.

Let $\tilde{H}_{f_c}(f)$ be the frequency response function of the band-pass filter, and let $\tilde{u}(f)$ be the Fourier transform of $u(t)$. The output voltage of the band-pass filter, $V(t; f_c)$, is expressed as

$$V(t; f_c) = \int_{-\infty}^{\infty} \tilde{H}_{f_c}(f) \tilde{u}(f) \exp(i2\pi f t) df \quad (4.2)$$

with

$$\tilde{u}(f) = \int_{-\infty}^{\infty} u(t) \exp(-i2\pi f t) dt. \quad (4.3)$$

The impulse response of the filter, $H_{f_c}(t)$, is given by

$$H_{f_c}(t) = \int_{-\infty}^{\infty} \tilde{H}_{f_c}(f) \exp(i2\pi f t) df. \quad (4.4)$$

Substituting Eqs. (4.3) and (4.4) into the rhs of Eq. (4.2), we obtain

$$V(t; f_c) = \int_{-\infty}^{\infty} H_{f_c}(t-t')u(t')dt' . \quad (4.5) \quad \text{form}$$

Since our experiment has been performed with the eight-pole Butterworth low- and high-pass filters, the argument of $\tilde{H}_{f_c}(f)$, f , can be replaced by f/f_c : $\tilde{H}_{f_c}(f) = \tilde{H}(f/f_c)$ (Fig. 1). Substituting $\tilde{H}(f/f_c)$ for $\tilde{H}_{f_c}(f)$ in the rhs of Eq. (4.4), one finds that $H_{f_c}(t) = f_c H(f_c t)$. Thereby, Eq. (4.5) is rewritten in the

$$V(t; f_c) = f_c \int_{-\infty}^{\infty} u(t') [H_{f_c}(t-t')] dt' . \quad (4.6)$$

This expression corresponds to the wavelet transform of $u(t)$.

If $t-t^{(i)} = t_i$, then the $2n$ th order moment $\langle [V(t; f_c)]^{2n} \rangle$ is expressed as

$$\langle [V(t; f_c)]^{2n} \rangle = \int_{-\infty}^{\infty} \cdots \int_{-\infty}^{\infty} f_c^{2n} \left\langle \prod_{i=1}^{2n} u(t-t_i) \right\rangle \prod_{i=1}^{2n} H(f_c t_i) dt_i . \quad (4.7)$$

Carrying out the scaling of f_c with λ , we have

$$\langle [V(t; \lambda f_c)]^{2n} \rangle = (\lambda f_c)^{2n} \int_{-\infty}^{\infty} \cdots \int_{-\infty}^{\infty} \left\langle \prod_{i=1}^{2n} u(t-t_i) \right\rangle \prod_{i=1}^{2n} H(\lambda f_c t_i) dt_i . \quad (4.8)$$

If $\lambda t_i = \tau_i$ and $\Delta\tau_{ij} = \tau_i - \tau_j$ for $i=1, 2, \dots, 2n$, then Eq. (4.8) gives

$$\langle [V(t; \lambda f_c)]^{2n} \rangle = f_c^{2n} \int_{-\infty}^{\infty} \cdots \int_{-\infty}^{\infty} G_{2n} \left[\frac{1}{\lambda} \Delta\tau_{ij} \right] \prod_{i=1}^{2n} H(f_c \tau_i) d\tau_i \quad (4.9)$$

with

$$G_{2n} \left[\frac{1}{\lambda} \Delta\tau_{ij} \right] = \left\langle u \left[t - \frac{\tau_1 - \tau_j}{\lambda} \right] u \left[t - \frac{\tau_2 - \tau_j}{\lambda} \right] \cdots u \left[t - \frac{\tau_{2n} - \tau_j}{\lambda} \right] \right\rangle . \quad (4.10)$$

Here, $\Delta\tau_{jj} = 0$, and G_{2n} is a $2n$ -point time correlation function of $u(t)$.

We postulate that the correlation function G_{2n} , in the statistical sense, has a scaling property insofar as f_c is located in the inertial range:

$$G_{2n} \left[\frac{1}{\lambda} \Delta\tau_{ij} \right] = \lambda^{-\xi_{2n}} G_{2n}(\Delta\tau_{ij}) , \quad (4.11)$$

where ξ_{2n} is the scaling exponent of the function G_{2n} . This assumption indicates that G_{2n} is a homogeneous function, such as $f(\lambda x) = g(\lambda) f(x)$ with $g(\lambda) = \lambda^s$, s being an arbitrary real number. Then, G_{2n} is assumed to be a self-similar function.

The scaling property of G_{2n} corresponds to that of the $2n$ th order structure function $\langle |u(t) - u(t - \Delta t)|^{2n} \rangle$, Δt being a time difference. There is, however, a great difference in that the $2n$ th order structure functions involve only two-point correlation functions $\langle u^s(t) u^{s'}(t - \Delta t) \rangle$, where $s + s' = 2n$ for $s, s' = 1, 2, \dots, 2n - 1$.

Substituting Eq. (4.11) into Eq. (4.9), we obtain from Eq. (4.7)

$$\langle [V(t; \lambda f_c)]^{2n} \rangle = \lambda^{-\xi_{2n}} \langle [V(t; f_c)]^{2n} \rangle . \quad (4.12)$$

This expression means that the moments $\langle [V(t; f_c)]^{2n} \rangle$, in the statistical sense, have a self-similar character, which is a feature of turbulent velocity in the inertial range.

If $\lambda f_c = f'_c$ in Eq. (4.12), we get $\langle [V(t; f_c)]^{2n} \rangle f_c^{\xi_{2n}} = \langle [V(t; f'_c)]^{2n} \rangle f'_c{}^{\xi_{2n}}$. Hence, we

have

$$\langle [V(t; \lambda f_c)]^{2n} \rangle = C_{2n} f_c^{-\xi_{2n}} , \quad (4.13)$$

C_{2n} being a constant. Thereby, Eq. (3.4) is rewritten in the form

$$\gamma_{2n} \propto f_c^{-n\xi_2 + \xi_{2n}} . \quad (4.14)$$

The scaling exponents ξ_{2n} are to be experimentally determined, but it becomes technically difficult to accurately determine ξ_{2n} for $2n > 12$. These results (4.13) and (4.14) were experimentally investigated.

We will remark on the following two cases, complete similarity (CS) and quasisimilarity (QS). (CS): The self-similarity is completely preserved under the assumption of the scaling transformation invariance (4.1):

$$\xi_{2n} = 2nh . \quad (4.15)$$

The statistics law of $V(t; f_c)$ is preserved for all f_c in the inertial range. (QS): The scaling exponent ξ_{2n} is a nonlinear function of order $2n$. The statistics law of $V(t; f_c)$ is never preserved, and it has the multifractal nature which is characteristic of three-dimensional turbulence.

Applying Eq. (4.15) to Eq. (4.14), one sees that γ_{2n} is independent of f_c : $\xi_{2n} - n\xi_2 = 0$. Then, the statistics law of $V(t; f_c)$ is preserved, and the sinusoidal variations of $V(t; f_c)$, therefore, must, in the statistical sense, be "completely" self-similar to each other among the ones with different values of f_c . On the other hand, in the case (QS), the statistics law is never preserved even in the inertial range; therefore, the stretching exponent m has to depend on f_c as shown in Fig. 4.

V. EXPERIMENTAL RESULTS

Figure 5 shows normalized one-dimensional energy-frequency spectra $E_1(f)/(v^3 k_d)$ obtained for the jet ($R_\lambda=270$) and the grid-produced turbulence ($R_\lambda=13$). Here, v is the kinematic viscosity of the fluid, and k_d is the Kolmogorov dissipation wave number. The magnitude of k_d was determined from the measured spectral distribution $E_1(f)$. The inertial range of $E_1(f)$ is roughly defined by f_0 and $f_d/10$, where $f_0=U_0/\Lambda$ with an integral scale Λ determined from the measured autocorrelation function of $u(t)$, and $f_d=U_0 k_d/2\pi$. Both ends of the inertial range have been marked with the arrows.

Figure 6 shows the log-log plots of γ_4 versus f_c/f_0 , for the turbulent flows with $R_\lambda=11-270$, where the arrows indicate the high-frequency ends of the inertial ranges, $f_d/(10f_0)$. Then, γ_4 was calculated from Eq. (3.4). When $R_\lambda > 40$, γ_4 has different features in three regions, which are the energy-containing range, the inertial range, and the dissipation range of $E_1(f)$.

In the energy-containing (integral-scale) range ($f_c > f_0$), γ_4 is nearly equal to 0.5, and $V(t;f_c)$ presents the Gaussian PDF as seen in Fig. 2(a). In the inertial range ($f_0 < f_c < f_d/10$), γ_4 decreases with increasing f_c . When $R_\lambda > 40$, $\log_{10}\gamma_4$ can be represented by a linear function of $\log_{10}(f_c/f_0)$: γ_4 has a scaling range in which the power law (4.14) holds. When R_λ is so small that $E_1(f)$ cannot have the inertial range, γ_4 has no scaling range. When R_λ is sufficiently large, G_4 is assumed to be asymptotically the homogeneous function. We will later have further discussion about this scaling property, including the higher orders of γ_{2n} .

In the dissipation range ($f_c > f_d/10$), γ_4 has no scaling property, and decreases rapidly with increasing f_c . Such rapid decreases indicate a remarkable change in the statistics law of $V(t;f_c)$. This is obvious from the fact that the stretching exponent m decreases more rapidly than in the inertial range (Fig. 4). It seems that the decrease in γ_4 is a little more rapid when R_λ is smaller.

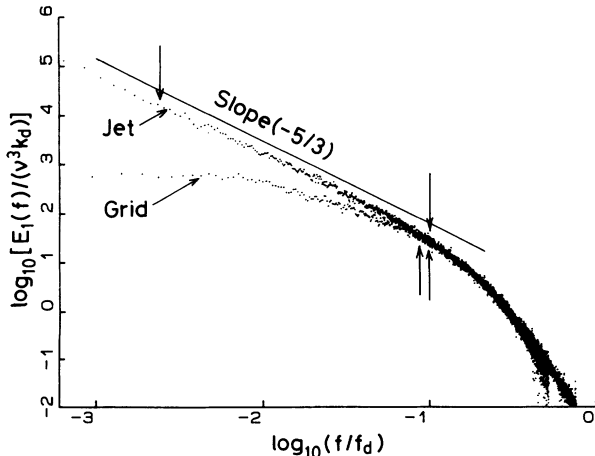


FIG. 5. Normalized one-dimensional energy-frequency spectra; jet ($R_\lambda=270$) and grid ($R_\lambda=13$) flows.

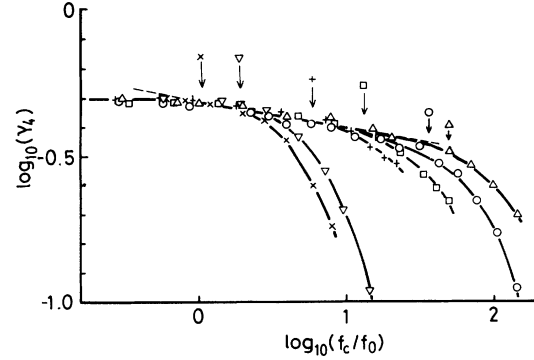


FIG. 6. Plots of γ_4 vs f_c/f_0 . Here, the arrows indicate the positions of $f_d/10$. (\circ) $R_\lambda=270$, $U_0=15$ m/s; (\triangle) $R_\lambda=124$, $U_0=24$ m/s; (\square) $R_\lambda=71$, $U_0=12.8$ m/s; ($+$) $R_\lambda=41$, $U_0=26.8$ m/s; (∇) $R_\lambda=11$, $U_0=3.1$ m/s; (\times) $R_\lambda=13$, $U_0=4.7$ m/s.

The change in the PDF is basically caused by the growth of quiescent parts such as those in Figs. 2(d) and 2(e).

Figure 7 shows the log-log plots of γ_{2n} versus f_c . The log-log plots have the linear region for all the given orders $2n$. The slopes of the straight lines are steeper in the higher orders. The ζ_{2n} exponents in Eq. (4.12) were determined from the linear region, but the ζ_2 exponent was calculated from the PDF.

Figure 8 shows the plots of ζ_{2n} as a function of $2n$, for the jet ($R_\lambda=270,66$) and the wake ($R_\lambda=124,71$) turbulent flows. These results have been compared with those of Anselmet *et al.* [19] for the velocity structure function. The scaling exponent ζ_{2n} is nonlinear for the order $2n$. We have the case (QS) realized. The inertial range intermittency of the band-pass signals asymptotically has the scaling property expressed by Eq. (4.14). The ζ_{2n} curves, including the one by Anselmet *et al.*, have a tendency to get nearer to the straight line of $\zeta_{2n}=2nh$ with the increase in R_λ . This suggests that the linear exponent $\zeta_{2n}=2nh$, the case (CS), is materialized in the limit $R_\lambda \rightarrow \infty$.

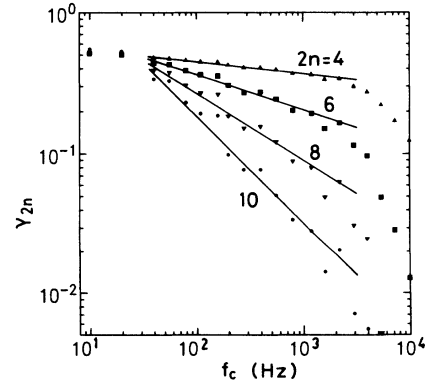


FIG. 7. Log-log plots of γ_{2n} vs f_c ; $R_\lambda=270$ jet flow at $U_0=15$ m/s.

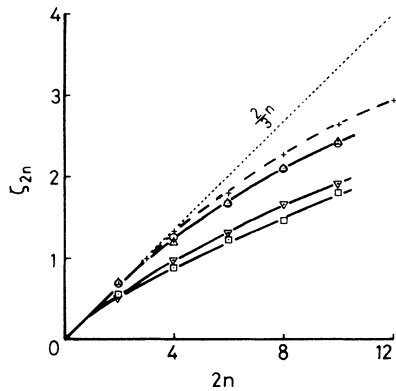


FIG. 8. Plots of ζ_{2n} vs $2n$; (+) scaling exponent ζ_{2n} of a structure function (Anselmet *et al.* [19], $R_\lambda=515$ duct flow); our experimental results; (\odot) $R_\lambda=270$, (\triangle) $R_\lambda=124$, (\square) $R_\lambda=71$, and (∇) $R_\lambda=66$.

VI. CONCLUDING REMARKS

We conclude from the experiments described above that the multifractal character (intermittency) is inherent in the scale-dependent deviation of the statistics law from the Gaussian process. The scale dependence of intermittency is classified into the three categories: (1) the (nearly) Gaussian process, (2) the non-Gaussian process, and (3) the spotty process.

(1) In the energy-containing range, the intermittency factors γ_{2n} are nearly equal to 0.5 at all given $2n$. The band-pass signals are nearly Gaussian. All the turbulent flows used in our experiment exhibited this Gaussian process irrespective of R_λ ($=11-270$). We must, however, add that it is very difficult to determine whether the randomly amplitude- and phase-modulated band-pass signals in this range are due to a mechanism of intermittency.

(2) In the inertial range, the band-pass signal becomes gradually more intermittent with increasing f_c , so the intermittency factors γ_{2n} decrease accordingly. The decreases in γ_{2n} obey the scaling law expressed by Eq. (4.14), and the inertial range intermittency is characterized by the scaling law.

The deviation of the PDF from the Gaussian statistics is characterized by the nonlinearity of the scaling exponent ζ_{2n} . This deviation, an inertial range attribute, refuses the homogeneous fractal leading to the linear exponent $\zeta_{2n}=2nh$. As shown by Benzi *et al.* [28] and Kailasnath, Sreenivasan, and Stolovitzky [29], the stretched exponential form of the PDF can be explained by the multifractal phenomenon. Thus, the behavior of the two exponents ζ_{2n} and m is related to the multifractal (intermittency) of turbulent velocity.

The decrease in the stretching exponent m with increasing f_c indicates that the envelopes of the band-pass

signals deform into sharper forms at larger amplitudes. The spottiness follows the sharpening of the envelopes, producing the dissipation range.

(3) In the dissipation range, the intermittency is the well-known spottiness, and the PDF continues deviating very greatly from the Gaussian with an increase in f_c . This range has no scaling property. The breakdown of the self-similarity accompanies the rapid decreases in γ_4 and m with increasing f_c , and brings about a drastic change in statistics law [Fig. 3 (d),(e)].

In the dissipation range, it is considered that the viscous effects on the turbulent fluid motion, the viscous energy dissipation, and the work by the viscous shear stress, bring about the drastic change in the statistics law. On the basis of the notion that the intermittency is accompanied by the change in the statistics law, it is quite natural that turbulence becomes notably intermittent in the dissipation scale range.

Complete self-similarity means that the linear scaling exponent $\zeta_{2n}=2nh$ underlies the scaling transformation invariance (4.1) in the limit $\nu \rightarrow 0$ (i.e., $R_\lambda \rightarrow \infty$). (As an aside, Kolmogorov's 1941 theory indirectly referred to the linear exponent, namely, to the "complete" self-similarity [31].) Since the fluid is viscous, the turbulent fluid motion cannot, even in the statistical sense, admit the completely self-similar structure.

The self-similarity (4.12) is asymptotically maintained in the inertial range in which the viscous effects are negligible. On the other hand, in the dissipation range, the viscous effects become important, and breakdown of the self-similarity (4.12) occurs. This breakdown becomes more noticeable for smaller scales in which the energy dissipation becomes more and more important.

Since a definite boundary cannot exist between the inertial range and the dissipation range, the spottiness of the band-pass signal begins to occur in the high-frequency side of the inertial range. The breakdown of the self-similarity, therefore, is not limited to within the dissipation range and begins more or less to occur in the inertial range. It is considered that the change in the statistics law is due to the fact that the Navier-Stokes equation for incompressible "viscous" fluid flows cannot be invariant under the scaling transformations (4.1).

In summary, intermittency describes the scale-dependent change in the statistics law. Our thought mentioned above has been already referred to in the previous papers about a hierarchical model [31,32].

ACKNOWLEDGMENTS

The wind tunnel used in the present study belongs to the Department of Civil Engineering of TMU. We wish to thank H. Yasukawa and M. Ui for willingly allowing us to use their laboratory and the wind tunnel.

- [1] G. K. Batchelor and A. A. Townsend, Proc. R. Soc. London Ser. A **199**, 238 (1949).
 [2] S. Pond and R. W. Stewart, Izv. Akad. Nauk SSSR, Fiz. Atmos. Okeana, **1**, 914 (1965).

- [3] C. H. Gibson, G. R. Stegen, and R. B. Williams, J. Fluid Mech. **41**, 153 (1970).
 [4] J. C. Wyngaard and H. Tennekes, Phys. Fluids **13**, 1962 (1970).

- [5] F. H. Champagne, *J. Fluid Mech.* **86**, 67 (1978).
- [6] C. W. Van Atta and R. A. Antonia, *Phys. Fluids* **23**, 252 (1980).
- [7] V. A. Sandborn, *J. Fluid Mech.* **6**, 221 (1959).
- [8] D. A. Kennedy and S. Corrsin, *J. Fluid Mech.* **10**, 366 (1961).
- [9] A. Y. -S. Kuo and S. Corrsin, *J. Fluid Mech.* **50**, 285 (1971).
- [10] A. N. Kolmogorov, *Dokl. Akad. Nauk SSSR* **30**, 301 (1941).
- [11] L. D. Landau and E. M. Lifshitz, *Fluid Mechanics* (Addison-Wesley, Reading, 1959).
- [12] A. M. Oboukhov, *J. Fluid Mech.* **13**, 77 (1962).
- [13] A. N. Kolmogorov, *J. Fluid Mech.* **13**, 82 (1962).
- [14] E. A. Novikov, *Prikl. Mat. Mekh.* **27**, 944 (1963).
- [15] E. A. Novikov and R. W. Stewart, *Izv. Akad. Nauk SSSR, Ser. Geofiz.* **3**, 408 (1964).
- [16] P. G. Saffman, *Phys. Fluids* **13**, 2193 (1970).
- [17] B. B. Mandelbrot, *J. Fluid Mech.* **62**, 331 (1974).
- [18] U. Frisch, P. -L. Sulem, and M. Nelkin, *J. Fluid Mech.* **87**, 719 (1978).
- [19] F. Anselmet, Y. Gagne, E. J. Hopfinger, and R. A. Antonia, *J. Fluid Mech.* **140**, 63 (1984).
- [20] C. Meaneveau and K. R. Sreenivasan, *Phys. Rev. Lett.* **59**, 1424 (1987); *Phys. Lett. A* **137**, 103 (1989); *J. Fluid Mech.* **224**, 429 (1991).
- [21] I. Hosokawa and K. Yamamoto, *Phys. Fluids A* **2**, 889 (1990).
- [22] R. Benzi, G. Paladin, G. Parisi, and A. Vulpiani, *J. Phys. A* **17**, 3521 (1984).
- [23] U. Frisch and G. Parisi, in *Turbulence and Predictability in Geophysical Fluid Dynamics*, edited by M. Gil, R. Benzi, and G. Parisi (North-Holland, Amsterdam, 1985).
- [24] C. Meaneveau and K. R. Sreenivasan, *Nucl. Phys. B* **2**, 49 (1987).
- [25] T. Nakano, *Phys. Lett. A* **140**, 395 (1989).
- [26] Z. -S. She, *Phys. Rev. Lett.* **66**, 600 (1991).
- [27] Z. -S. She, E. Jackson, and S. A. Orszag, *J. Sci. Comput.* **3**, 407 (1988).
- [28] R. Benzi, L. Biferale, G. Paladin, A. Vulpiani, and M. Vergassola, *Phys. Rev. Lett.* **67**, 2299 (1991).
- [29] P. Kailasnath, K. R. Sreenivasan, and G. Stolovitzky, *Phys. Rev. Lett.* **68**, 2766 (1992).
- [30] U. Frisch, *Proc. R. Soc. London Ser. A* **434**, 89 (1991).
- [31] K. Nagata and T. Katsuyama, *Physica (Utrecht) A* **188**, 607 (1992).
- [32] K. Nagata and T. Katsuyama, *Physica (Utrecht) A* **155**, 585 (1989).